Photoemission Spectroscopy and X-ray Absorption Spectroscopy Studies of the Superconducting Pyrochlore Oxide Cd2Re207

Irizawa, Akinori ; Higashiya, A. ; Kasai, S. ; Sasabayashi, T. ; Shigemoto, A. ; Sekiyama, A. ; Imada, S. ; Suga, S. ; Sakai, H. ; Ohno…

(Citation)
Journal of the Physical Society of Japan,75(9):94701-94701

(Issue Date)
2006-09

(Resource Type)
journal article

(Version)
Accepted Manuscript

(URL)
https://hdl.handle.net/20.500.14094/90000174

Photoemission spectroscopy and X-ray absorption spectroscopy studies of the superconducting pyrochlore oxide $Cd_2Re_2O_7$

A. Irizawa*, A. Higashiya†, S. Kasai, T. Sasabayashi, A. Shigemoto, A. Sekiyama, S. Imada, S. Suga, H. Sakai[1‡], H. Ohno[1], M. Kato[1§], K. Yoshimura[1] and H. Harima[2]

Division of Materials Physics, Graduate School of Engineering Science, Osaka University, Osaka 560-8531, Japan

[1]*Department of Chemistry, Graduate School of Science, Kyoto University, Kyoto 606-8502, Japan*

[2]*Department of Physics, Faculty of Science, Kobe University, Hyogo 657-8501, Japan*

Photoemission spectroscopy (PES) and O 1*s* X-ray absorption spectroscopy (XAS) measurements have been performed for $Cd_2Re_2O_7$ single crystals. Temperature variations of their spectra reveal that the phase transition at 120 K directly changes the band structure near the Fermi level compared with another transition near 200 K. The roles of the transitions are discussed in terms of the changes in the Re-O orbital hybridization.

KEYWORDS: pyrochlore, $Cd_2Re_2O_7$, PES, XAS

1. Introduction

$Cd_2Re_2O_7$ was found to be a superconductor[1)–3)] ($T_c \sim 1$ K) as the first case among the large family of pyrochlore oxides with the formula unit of $A_2B_2O_7$ (typically, A=rare earth or late transition metal, B=3*d*, 4*d* and 5*d* transition metal).[4)] In this compound, A and B cations, namely A=Cd and B=Re, are 2- and 6-coordinated by the nearest oxygen anions. The oxygen centered $[\frac{1}{2}A]_4$-O tetrahedrons are connected as forming a pyrochlore lattice with straight O-A-O bonds, while the B cation centered B-$[\frac{1}{2}O]_6$ octahedrons form a pyrochlore lattice with the bent B-O-B bonds with the angle in the range of 110∼140°. In the case of magnetic B cations, the deviation from the straight alignment in B-O-B bond enables the existence of magnetic fluctuation because of the competition between the ferromagnetic and antiferromagnetic exchange interactions among the B cations. Assuming the electronic configurations in $Cd_2Re_2O_7$ as formally Cd^{2+} ($4d^{10}$) and Re^{5+} ($4f^{14}5d^2$), the electronic and magnetic properties are thought to be primarily dominated by the Re 5*d* electrons near the Fermi level. Such an electronic structure in this compound is predicted by the band calculations,[5),6)] and observed in the photoemission studies.[7),8)] Above T_c, $Cd_2Re_2O_7$ shows anomalies in the elec-

*Present address: Graduate School of Science and Technology, Kobe University, Hyogo, Japan.
†Present address: SPring-8 / RIKEN, Hyogo, Japan
‡Present address: Advanced Science Research Center, Japan Atomic Energy Research Institute, Ibaraki, Japan
§Present address: Department of Molecular Science and Technology, Faculty of Engineering, Doshisya University, Kyoto, Japan

tric resistivity, magnetic susceptibility, specific heat, Hall coefficient, thermoelectric power, magnetoresistance and elastic moduli near 120 and/or 200 K.[1),2),9)–12)] Above and below 120 and 200 K, XRD, NMR, NQR, and Raman scattering studies have been taken place with a view to reveal the details of atomic conformation in each phase.[13)–19)] The single-crystal X-ray diffraction studies indicate that the transition near 200 K is a second-order structural phase transition with changing its crystallographic symmetry from an ideal cubic $Fd\bar{3}m$ to a lower symmetry tetragonal $I\bar{4}m2$ representation with lowering temperature.[13)–15)] Gradual changes of ^{111}Cd NMR spectra through 200 K also infer the second-order structural transition.[16)] Although the driven force of this transition is not clear yet, it gives rise to the distinct change in the electric resistivity and the magnetic susceptibility.[1),2),17)] The electric resistivity is almost temperature independent around 300 K and drops abruptly below 200 K. The magnetic susceptibility shows a weak temperature dependence of Curie-Weiss type above ~400 K, takes a broad maximum near 290 K and steeply decreases below 200 K.

At around 120 K, the other phase transition with the first order character[18)] leads to another tetragonal space group $I4_122$ with lowering temperature accompanied by a small hysteresis in the electric resistivity.[11)] This is also notable transition as to correlate with a possible electronic structural change at the Fermi level. In both specific heat and thermoelectric power, an anomaly is observed as a kink at this temperature, whereas the magnetic susceptibility shows no significant change.[1),9),10)] ^{185}Re and ^{187}Re NQR spectra point out no magnetic order down to 5K.[16),18)] The relative magnetoresistance $\Delta\rho/\rho_0$ exhibits finite values between 100 and 200 K with such an anisotropy as positive for [001], nearly zero for [111], and even slightly negative for [110] direction. The whole magnetoresistances once converge to zero with decreasing temperature down to 100 K, but rapidly increases below this temperature up to 30 % at 2 K.[11)] The alteration of the structure through these two phase transitions is disscussed in the view of motions of oxygen ions constituting ReO_6 octahedra or Cd-O network from the polarized Raman scattering.[19)]

In this paper, we report on the results of photoemission spectroscopy (PES) for the occupied states and O 1*s* X-ray absorption spectroscopy (XAS) for the unoccupied states in order to get further understanding of the phase transitions near 120 and 200 K in $Cd_2Re_2O_7$.

2. Experimental

The measurements were performed by using synchrotron radiation at the beam line BL25SU in SPring-8 with a Scienta SES200 electron analyzer. The excitation photon energies were set to 935 eV for the PES measurements to be free from possible overlap of Auger spectra and in the range of 600~1100 eV for the check of surface contributions in the spectra. The overall energy resolution was set to be better than 80 meV for the PES near E_F and better than 200 meV for the wide valence band and the core level photoemission. The O 1*s* XAS measurements were performed in the total electron yield mode. Both measurements were

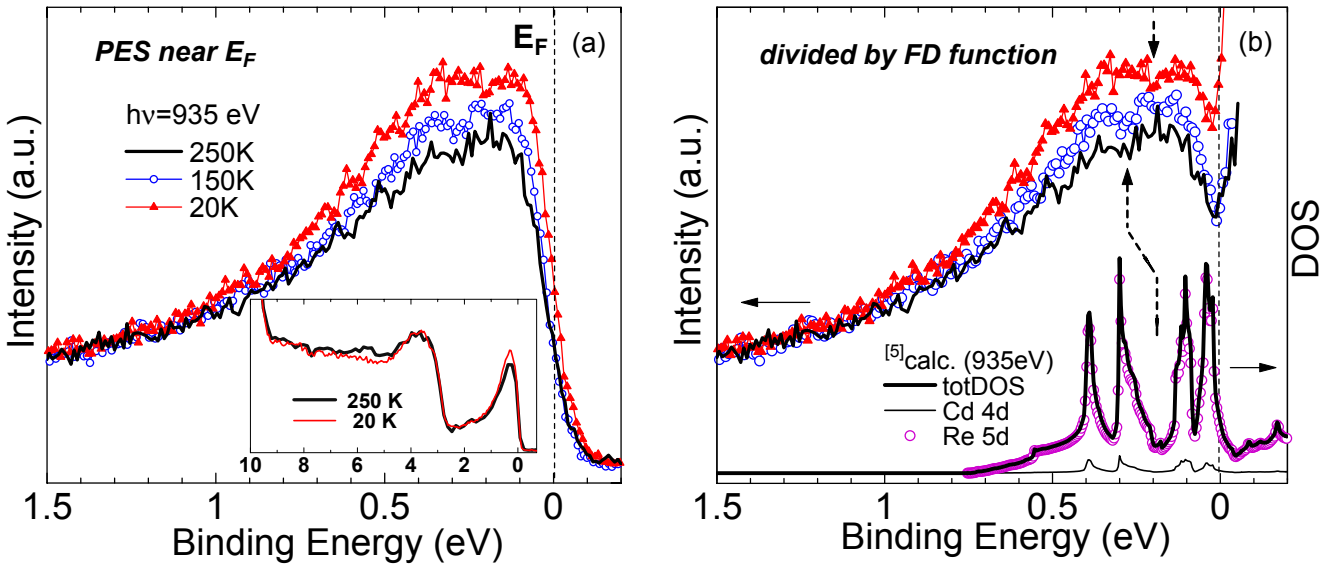

Fig. 1. (a) Temperature variations of the PES spectra at hν=935 eV near E_F and valence band. (b) Experimental spectra divided by the Fermi-Dirac function convoluted with the Gaussian FWHM of 80 meV corresponding to the instrumental resolution. They are compared with the band calculation at 300 K.[5] The total DOS and PDOSs are represented by 2 different curves and 1 dots. The PDOSs of O 2p states are very weak so as to be negligible.

done at 20, 150 and 250 K below and above the transition temperatures of 120 and 200 K. Clean surfaces for the measurements were obtained by cleaving single-crystal samples *in situ* under an ultra-high vacuum of better than 5×10^{-8} Pa. The obtained crystal surfaces were certified as the (111) face by the Laue diffraction patterns.

3. Results and Discussion

3.1 Photoemission spectra

Figure 1(a) shows the temperature variation of the photoemission spectrum near the Fermi level and the wide valence band shown in the inset. All the PES spectra show finite intensity at E_F related to the metallic conduction. In the wide range valence band spectra, the spectral weight near E_F increases and between 4.8 and 7.5 eV decreases with decreasing temperature. The significant change in the valence band was confined to the shown energy region as the inset. The total spectral weight is compensated in the valence band region through the experimental temperature range. The band calculation at 300 K predicts the gap between 0.7 and 2.3 eV as a result of the difference of energy level between the Re 5d and O 2p states.[5] This gap has been enhanced by the large hybridization between them. The valence and conduction bands are clearly separated by this gap as the bonding and anti-bonding states. The valley structure around 2 eV observed in PES spectra corresponds to this gap. Thus, the Fermi level is predicted in the bottom of the anti-bonding state.

The temperature variation of DOS near the Fermi level is carefully checked after a division by the Fermi-Dirac (FD) function including the instrumental energy resolution in Figure 1(b). The empirical procedure is employed by introducing an effective temperature $T_{eff} = \sqrt{T^2 + (\Delta E^{\rm exp}/4k_B)^2}$ to the FD function, where the line broadening due to the resolution limit can be taken into account by adopting the full width at half maximum (FWHM) of the Gauss function as $\Delta E^{\rm exp}$.[20] As a result, the spectral intensity at $E_{\rm F}$ is comparable between 150 and 250 K as opposed to the critical change in the electric resistivity across the phase transition at 200 K.[1),2)] However, the dip structure just below $E_{\rm F}$ at 20 K is much smaller than that at 150 and 250 K. In contrast, the photoemission study at the photon energy of 21.218 eV (He Iα) has concluded that the change in DOS near $E_{\rm F}$ at 100 K with respect to that at 300 K is less than 5% and is negligible.[7)] Another experiment of STS and low-photon energy PES resulted in the similar tendency of DOS variations to ours,[21)] but, it should be awared that the contribution of O 2p in PES spectra is comparable to that of Re 5d and *primarily* surface-sensitive in the low-photon energy experiments. The band calculation shown in Fig. 1(b) was performed by using a full potential FLAPW method with the local density approximation (LDA) for the ideal cubic $Fd\overline{3}m$ phase at around room temperature.[5)] Each partial DOS (PDOS) of the band calculation result has been weighted according to the cross-sections[22)] at the photon energy of 935 eV in this figure. According to this, Re 5d states are dominant in the total DOS near the Fermi level as demonstrated by the open dots in the figure. In the experimental spectra, rather complex peak structures are observed in the range of 100$\sim$400 meV at all temperatures of 20, 150 and 250 K. Considering the statistics of the experiment, these peaks seem to be separated into two parts at the energies indicated by the dashed arrows. This feature corresponds well to the split peak structures in the calculation result. The change of the split position stands out between 20 K and the other higher temperatures. The spectral shape in the peak region seems to be larger changed between 20 and 150 K rather than between 150 and 250 K.

Among inner core photoemission spectra, only the Re 4f spectrum has shown noticeable temperature dependence[8)] as reproduced in Figure 2(a). In addition to the J=7/2 and 5/2 spin-orbit split components, a prominent shoulder structure is observed at higher binding energies. The spectral weight transfers from the shoulder to the peak structures with decreasing the temperature. This shoulder structure cannot be simply ascribed to only single set of the J=7/2 and 5/2 components. The intensity around 43 and 46 eV in this broad shoulder structure shows hν dependence between 600 and 1100 eV influenced by the difference of the mean free path. This result strongly suggests the existence of the measurable surface components at around 43 and 46 eV split by the spin-orbit interaction. It should be emphasized that this shoulder structure is *never* derived from a degradation of the surface as a oxidation. The O 1s spectrum do not show any change through the experiment.[8)] Meanwhile, the Re NQR spectra denote

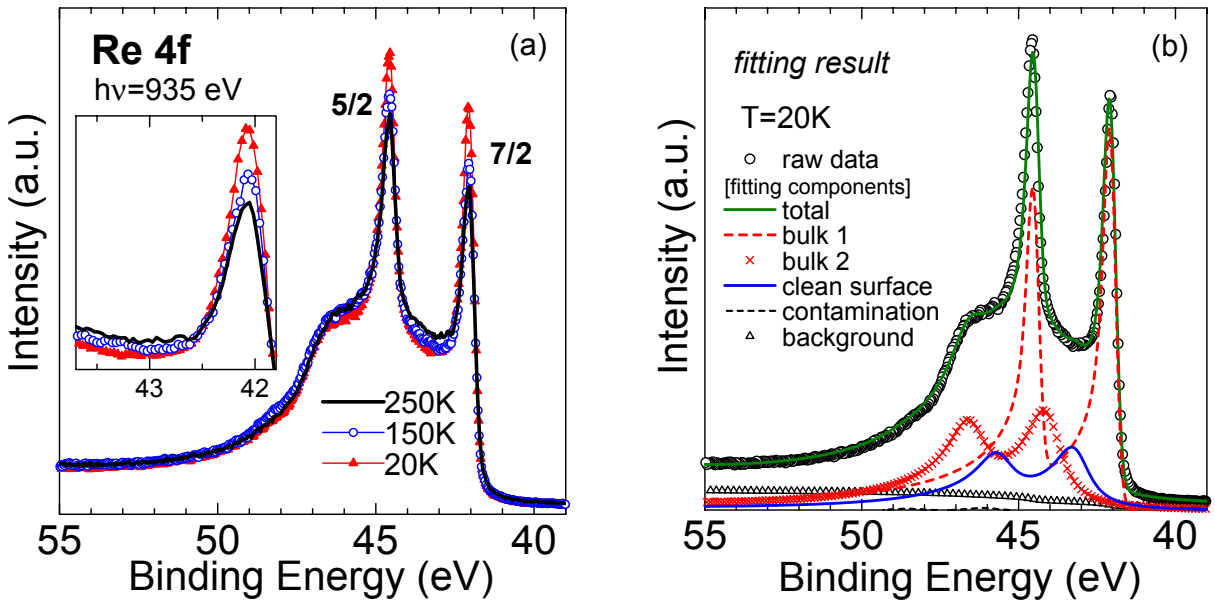

Fig. 2. (a) Temperature variation of the Re $4f$ spectra normalized by the summarized intensity of the bulk components ('bulk 1' and 'bulk 2'). (b) Typical analysis of the Re $4f$ inner core photoemission spectrum is shown for 20 K. Four spin-orbit split doublet components are employed for the deconvolution. The bulk components 'bulk 1' stands for the main peak (well screened) and 'bulk 2' represents the satellite peak (poorly screened). The 'clean surface' represents the intrinsic surface component on the cleaved surface, while the 'background' comes from a contribution of secondary electrons.

that the low temperature phase below 120 K exhibits the absence of any magnetic ordering and inhomogeneous valence in Rhenium. This result rules out the possibility of multi components in the Re $4f$ inner core photoemission spectra due to the different electronic states. In Figure 2(b) is reproduced the Re $4f$ spectra at 20 K, together with the result of deconvolution with assuming 4 sets of spin-orbit split components. The component 'bulk 1' represents the main sharp peak (well screened), the 'bulk 2' stands for a satellite peak (poorly screened), the 'clean surface' component is present just after cleaving samples *in situ*. All the asymmetric parameters are less than 0.3. The deconvolution was not able to be enforced only in 3 sets or less of components by any means. The background is coming from the secondary electrons. Among them, both 'bulk 1' and 'bulk 2' components are thought to be bulk-derived.

Table 1 summarizes the results of deconvolution analysis for 20, 150 and 250 K with respect to the binding energies and relative intensities where the intensity of the bulk components amounts to 1.00 in each temperature. Judging from these results, the spectral weight transfers from the 'bulk 2' to the 'bulk 1' component by about 8 % with decreasing temperature from 250 to 20 K. When we employ the nominal value of Re^{5+} ($5d^2$) state in this system, the main peak corresponds to the photoemission final state of $5d^3\underline{L}$ and the satellite to $5d^2$. The increase

	20K		150K		250K	
ID	B.E. (eV)	R.I. (ratio)	B.E. (eV)	R.I. (ratio)	B.E. (eV)	R.I. (ratio)
bulk 1 (bulk)	42.03	0.62	42.03	0.58	42.03	0.54
clean surface (surface)	43.15	0.24	43.15	0.23	43.02	0.24
bulk 2 (bulk)	44.05	0.38	44.05	0.42	43.92	0.46

Table I. Binding energy (B.E.) and relative intensity (R.I.) of each component obtained from the deconvolution of Re $4f$ inner core spectrum. The sum of intensities is set to 1.00 for the bulk components, i.e. $[bulk1] + [bulk2] = 1.00$, in each temperature.

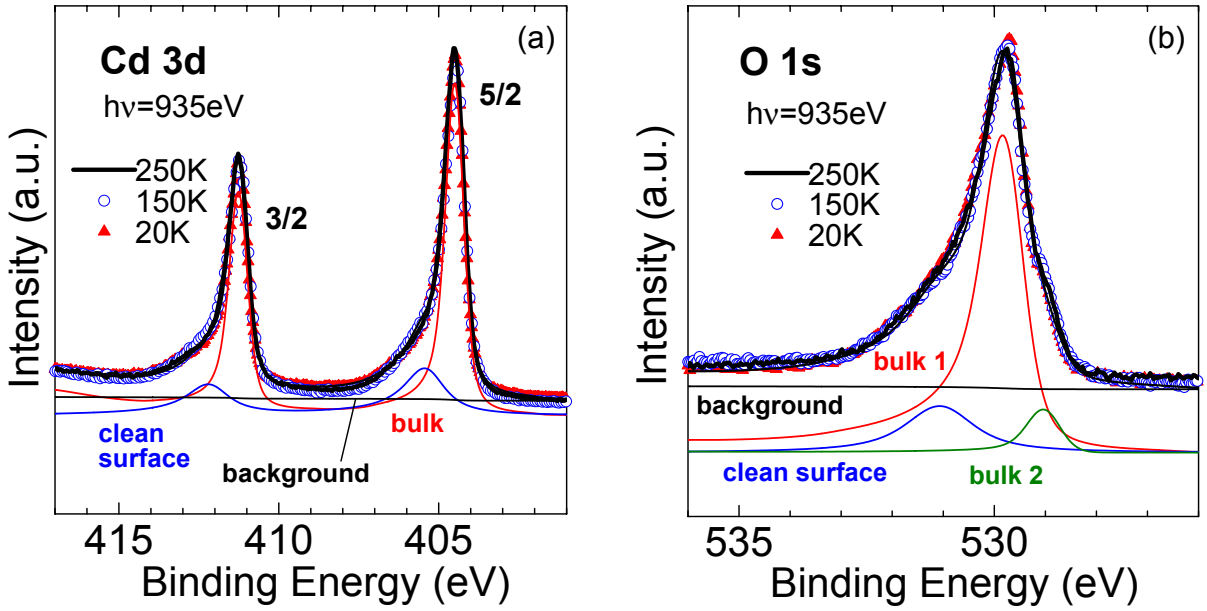

Fig. 3. Temperature variation of the Cd 3d (a) and O 1s (b) inner core photoemission spectra with the results of deconvolution by considering the components of bulk, clean surface and background. Additional component exists on the higher binding energy side of the main peak in the O 1s spectra.

of the main peak with decreasing temperature denotes the increase of charge transfer from the ligand (L), i.e. oxygen, to the Re site at lower temperatures. In contrast, the intensity of the 'clean surface' components stays almost constant in the temperature region of 20∼250 K within few hours during the experimental procedure.

The Cd 3d and O 1s inner core spectra do not show any meaningful change through 20, 150 and 250 K as shown in Fig. 3(a) and (b). All spectra are also explained by considering the 'bulk' and 'clean surface' components. One can notice an additional satellite or a shoulder (bulk 2) on the lower binding energy side of the main peak (bulk 1) in the case of the O 1s spectra. The structures of 'bulk 1' and 'bulk 2' may be resulting from the existence of

the two different crystallographic sites of oxygen associated with the Re-$[\frac{1}{2}O]_6$ octahedrons (O(1) site) and $[\frac{1}{2}Cd]_4$-O tetrahedrons (O(2) site). Considering the composition ratio, the oxygen numbers in the octahedral and tetrahedral networks are 6 and 1 for O(1) and O(2) in the formula of $Cd_2Re_2O_7$.[4),26)] The intensity of the satellite structure 'bulk 2' in the O 1s spectrum is about 0.1 of the main peak 'bulk 1', that is comparable to the site occupancy ratio of O(2)/O(1)=1/6.

3.2 X-ray absorption spectra

In order to probe the unoccupied electronic states of this compound, O 1*s* XAS measurement was performed at 20, 150 and 250 K. Figure 4(a) summarizes the temperature variation of the O 1*s* XAS spectra compared with the result of band calculation at 300 K. All the experimental spectra are normalized at the intensity of the peak at around hν=-13.5 eV in the figure. Although the origin of this peak is not clarified yet by the calculation available between -10 and 10 eV, the shape of this peak is simple and almost unchanged at all temperatures. It is conjectured that this peak structure originates from the part of oxygen *p* state without substantial hybridization with the Cd or Re orbital and shows only poor temperature dependence. In the region from -10 to 0 eV, the spectral shapes and peak positions of the experimental results are in a qualitative agreement with the calculated result. As for the temperature variation, we can recognize a clear change between 20 and 150 K in contrast to the slight change between 150 and 250 K.

According to the simplified band picture represented in Figure 4(b), it is possible that the region of -2 to 1 eV corresponds to the π-like anti-bonding state (π*) and the region of -10 to -4 eV is ascribed to the σ-like anti-bonding state (σ*). The gap between the bonding and anti-bonding states is opened on the basis of the energy separation between the Re 5*d* and O 2*p* orbitals, where the σ- and π-like states are derived from the strong and weak hybridizations between them. Therefore, the temperature change from 150 to 20 K in the XAS spectra must be expressed as that the O 2*p* PDOS in the π* state is decreased and that in the σ* state is increased as shown in the right part of Fig. 4(b). At the same time, it is consistent with the change of the photoemission spectra across 120 K in a sense that the DOS near E_F, mostly reflecting the Re 5*d* PDOS in the π* state, is increased at lower temperatures. These facts conclude that the occupancy of O 2*p* orbital in the π* state is much more attenuated below 120 K. In respect of bonding state, although the change of the valence band photoemission spectra around 6 eV may also correspond to the series of these spectral transformations, such a simplified band picture is no more suitable for the occupied state because of the large hybridization. The systematic band calculation for each temperature has not been executed because the uncertainty of the lattice constants at lower temperatures,[13)–15)] but the phase transition near 120 K is ascertained as the critical change in the [Re 5*d*]-[O 2*p*] hybridization which implies the realignment of the angle and/or length of the Re-O bond involving the

electronic band structure near the Fermi level. On the contrary, the transition near 200 K turns out less sensitive to the electronic band structure near E_F from this study.

Finally, we try to give a picture of these complex phase transitions with an eye to other experiments. The results of PES and XAS studies contradict the conclusion presented in the NMR study,[23] where they have assumed that the DOS at the Fermi level would decrease below 200 K. One of the possible explanation is that the sudden decreases of the spin susceptibility and ^{111}Cd $(T_1T)^{-1}$ may arise from the suppression of spin fluctuation below 200 K. The transition at around 200 K is expected to involve the freezing of a kind of lattice breathing mode in accordance with the spin singlet formation below 200 K.[13] It could be associated with the change of the motion of oxygen ions in ReO_6 octahedra.[19] The decrease of resistivity below 200 K can be explained by the diminution of the electron scattering originating in the magnetic fluctuation. In that sense, the transition at around 200 K is not necessarily sensitive to PES and XAS experiments. On the other hand, the increase of DOS at E_F with decreasing temperature from 150 to 20 K will originate from the change of the hybridization between the Re 5*d* and O 2*p* orbits across the first-order phase transition at 120 K.[11] It should be noted that the similar change of DOS is also led from the optical study.[24] Although the optical conductivity exhibits the complicated spectra at lower frequency, the reflectivity shows the apparent change only from 150 to 24 K: the value increases toward 1 at the lowest frequency, and the redistribution of spectral weight reflecting the change of band structure is observed up to midinfrared region.

For the lower temperature phases, the displacements of the Re and the O(1) atoms from the ideal position in the pyrochlore structure have been examined closely on the ground of the group theoretical analysis of phonons.[25] Although it does not mention the changes of the band structure, someone may develop soon. These characteristic features in the normal state are important to better understand the origin of the superconducting transition in this compound.

4. Conclusion

The temperature dependence of the PES and O 1*s* XAS are investigated in $Cd_2Re_2O_7$ by using soft X-ray synchrotron radiation. A clear temperature change is found in the Re 4*f* inner core spectra which is correlated with the Re 5*d* states dominating near the Fermi level. Both occupied and unoccupied valence band spectra near the Fermi level observed by PES and XAS studies are sensitive for the phase transition near 120 K rather than that near 200 K. In the occupied state, the increase of the DOS and the change of the peak structure are observed near the Fermi level where the Re 5*d* states dominate in PES at the photon energy of 935 eV. Corresponding critical change across 120 K is also seen for the unoccupied state probed by the O 1*s* XAS. The decrease of oxygen PDOS in the π^* bond with decreasing temperature is consistent with the increase of Re PDOS. These results strongly imply the

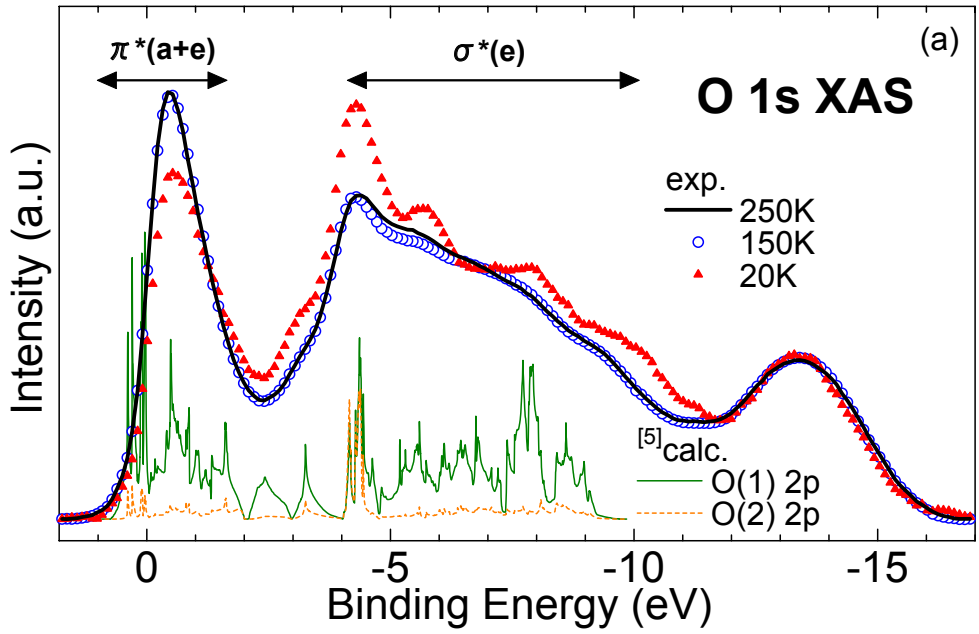

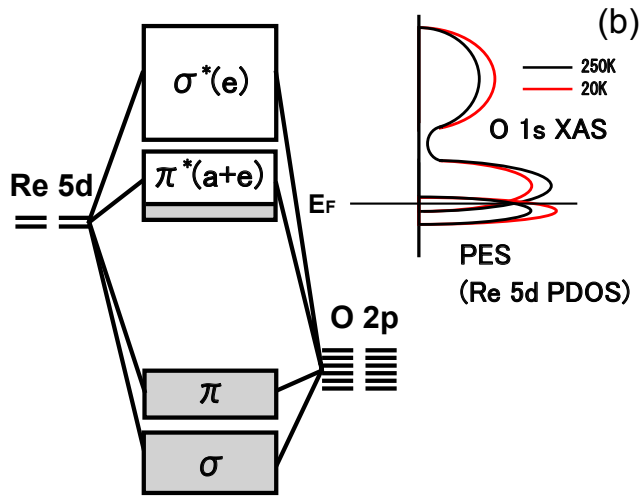

Fig. 4. (a) Temperature variation of the O 1*s* XAS spectra normalized by the intensity of the peak structure at around -13.5 eV. The O(1) and O(2) PDOS in the calculation result at 300 K are drawn by the thin lines for comparison.[5)] (b) Schematic band structure of $Cd_2Re_2O_7$ near the Fermi level. Two Re 5*d* and six O 2*p* orbitals as forming the Re-O(1) network in the formula unit are considered. The shaded area indicates the occupied state. The Fermi level is located at the bottom of the π anti-bonding state. Right hand illustration denotes the relative change of O 1*s* XAS and PES spectra in the anti-bonding state with temperature variation.

reduction in the Re-O π bond hybridization below 120 K.

Acknowledgments

We are grateful to Dr. T. Muro and Dr. Y. Saitoh of SPring-8 for their generous supports for the experiment. The research was performed at SPring-8 under the support of a Grant-in-Aid for the COE Research (10CE2004) of the Ministry of Education, Culture, Sports, Science, and Technology (MEXT), Japan.

References

1) M. Hanawa, Y. Muraoka, T. Tayama, T. Sakakibara, J. Yamaura, and Z. Hiroi : Phys. Rev. Lett. **87** (2001) 187001.
2) H. Sakai, K. Yoshimura, H. Ohno, H. Kato, S. Kambe, R E. Walstedt, T D. Matsuda, Y. Haga, and Y. Onuki : J. Phys. Cond. Matter. **13** (2001) L785.
3) R. Jin, J. He, S. McCall, C.S. Alexander, F. Drymiotis, and D. Mandrus : Phys. Rev. B **64** (2001) 180503.
4) M.A. Subramanian, G. Aravamudan, and G.V.S. Rao : Prog. Solid St. Chem. **15** (1983) 55.
5) H. Harima : J. Phys. Chem. Solids. **63** (2002) 1035.
6) D.J. Singh, P. Blaha, K. Schwarz, and J.O. Sofo : Phys. Rev. B **65** (2002) 155109.
7) R. Eguchi, T. Yokoya, T. Baba, M. Hanawa, Z. Hiroi, N. Kamakura, Y. Takata, H. Harima, and S. Shin : Phys. Rev. B **66** (2002) 012516.
8) A. Irizawa, A. Higashiya, S. Kasai, T. Sasabayashi, A. Shigemoto, A. Sekiyama, S. Imada, S. Suga, H. Sakai, H. Ohno, M. Kato, and K. Yoshimura : Acta Phys. Pol. B (conference proceedings of SCES2002, Krakow) **34** (2003) 553.
9) R. Jin, J. He, J.R. Thompson, M.F. Chisholm, B.C. Sales, and D. Mandrus : J. Phys. Cond. Matter. **14** (2002) L117.
10) D. Huo, A. Mitsuda, Y. Isikawa, J. Sakurai, H. Sakai, H. Ohno, M. Kato, K. Yoshimura, S. Kambe, and R.E. Walstedt : J. Phys. Cond. Matter. **14** (2002) L257.
11) Z. Hiroi, J. Yamaura, Y. Muraoka, and M. Hanawa : J. Phys. Soc. Jpn. **71** (2002) 1634.
12) I.A. Sergienko, V. Keppens, M. McGuire, R. Jin, J. He, S.H. Curnoe, B.C. Sales, P. Blaha, D.J. Singh, K. Schwarz, and D. Mandrus : Phys. Rev. Lett. **92** (2004) 65501.
13) M. Hanawa, J. Yamaura, Y. Muraoka, F. Sakai, and Z. Hiroi : J. Phys. Chem. Solids. **63** (2002) 1027.
14) J. Yamaura, and Z. Hiroi : J. Phys. Soc. Jpn. **71** (2002) 2598.
15) J.P. Castellan, B.D. Gaulin, J. van Duijn, M.J. Lewis, M.D. Lumsden, R. Jin, J. He, S.E. Nagler, and D. Mandrus : Phys. Rev. B **66** (2002) 134528.
16) O. Vyaselev, K. Kobayashi, K. Arai, J. Yamazaki, K. Kodama, M. Takigawa, M. Hanawa, and Z. Hiroi : J. Phys. Chem. Solids. **63** (2002) 1031.
17) H. Sakai, H. Kato, S. Kambe, R.E. Walstedt, H. Ohno, M. Kato, and K. Yoshimura : Phys. Rev. B **66** (2002) 100509R.
18) K. Arai, K. Kobayashi, K. Kodama, O. Vyaselev, M. Takigawa, M. Hanawa, and Z. Hiroi : J. Phys.: Condens. Matter **14** (2002) L461.
19) C.S. Knee, J. Holmlund, J. Andreasson, M. Käll, S.G. Eriksson, and L. Börjesson : Phys. Rev. B **71** (2005) 214518.
20) T.J. Kreutz : PhD thesis, University of Zürich. (1997).
21) Chenxi Lu, Jiandi Zhang, R. Jin, Hongwei Qu, J. He, D. Mandrus, Ku-Ding Tsuei, Chuan-Tze Tzeng, Li-Cheng Lin, and E.W. Plummer : Phys. Rev. B **70** (2004) 92506.
22) J.J. Yeh, and I. Lindau : At. Data Nucl. Data Tables **32** (1985) 1.
23) O. Vyaselev, K. Arai, K. Kobayashi, J. Yamazaki, K. Kodama, M. Takigawa, M. Hanawa, and Z. Hiroi : Phys. Rev. Lett. **89** (2002) 017001.
24) N.L. Wang, J.J. McGuire, T. Timusk, R. Jin, J. He, and D. Mandrus : Phys. Rev. B **66** (2002)

14534.
25) I.A. Sergienko, and S.H. Curnoe : J. Phys. Soc. Jpn. **72** (2003) 1607.
26) Z. Hiroi, and M. Hanawa : J. Phys. Chem. Solids. **63** (2002) 1021.

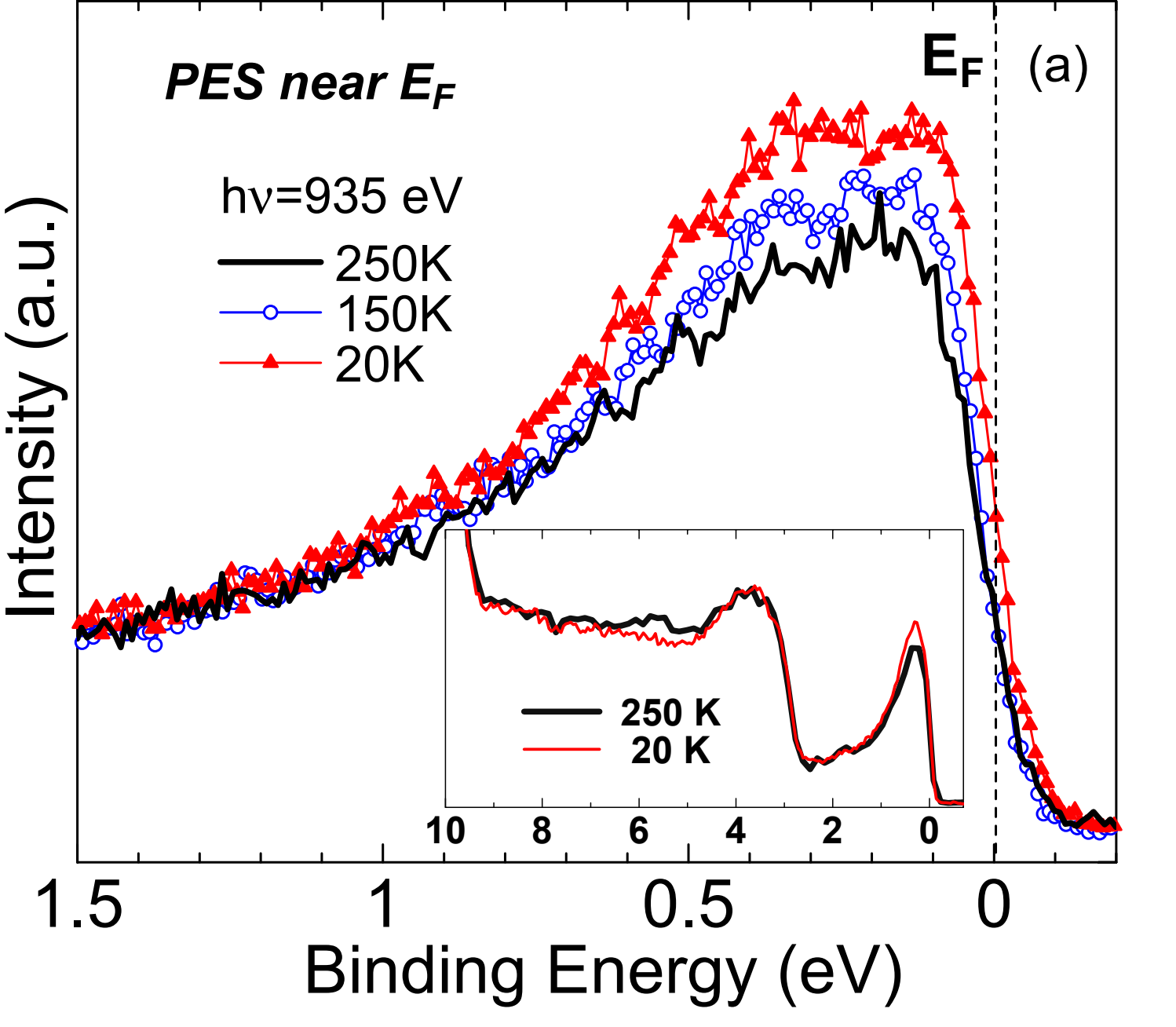
PES near E_F
E_F
(a)
hν=935 eV
250K
150K
20K
Intensity (a.u.)
250 K
20 K
10
8
6
4
2
0
1.5
1
0.5
0
Binding Energy (eV)

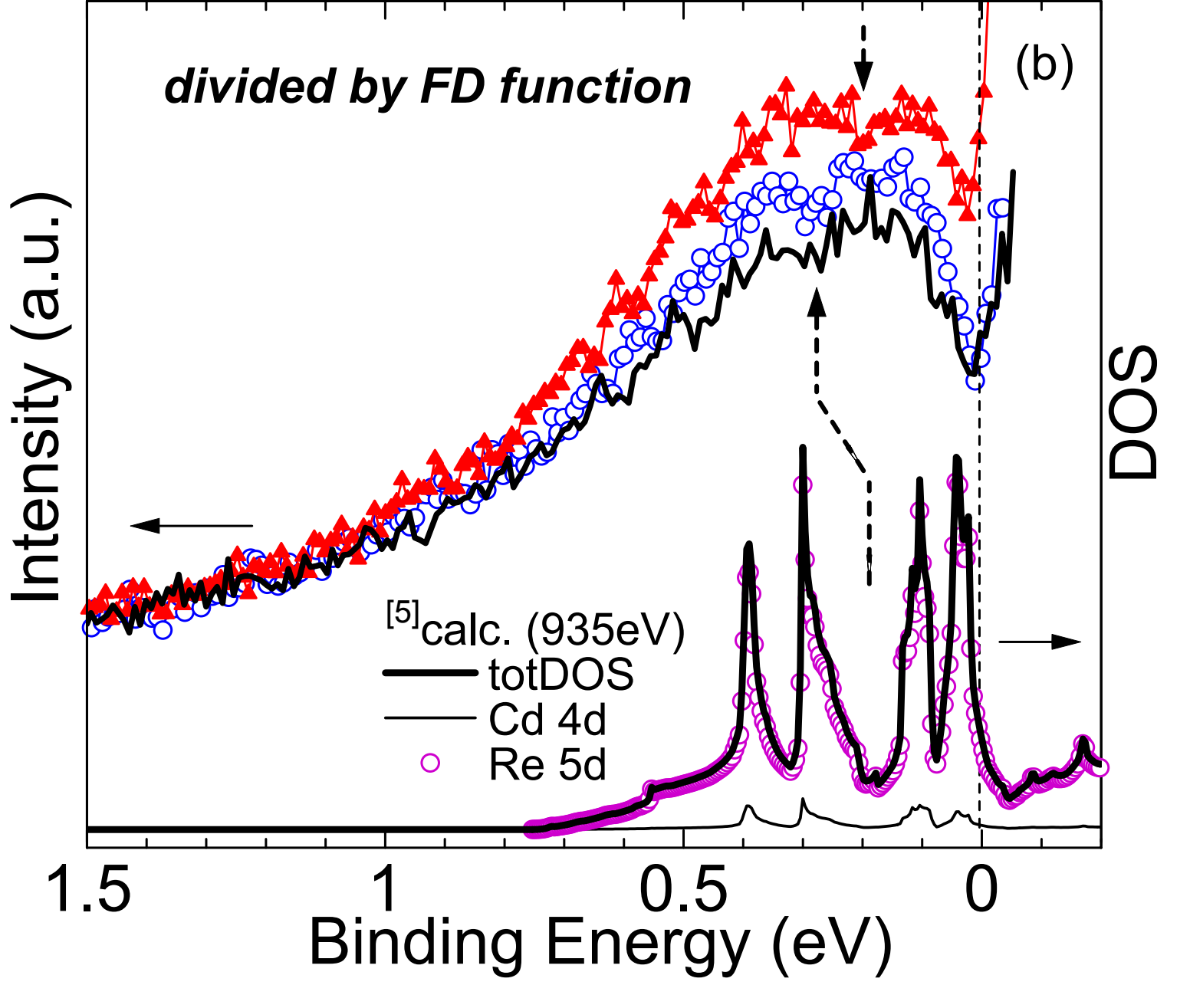
divided by FD function
(b)
Intensity (a.u.)
DOS
[5]calc. (935eV)
totDOS
Cd 4d
Re 5d
1.5
1
0.5
0
Binding Energy (eV)

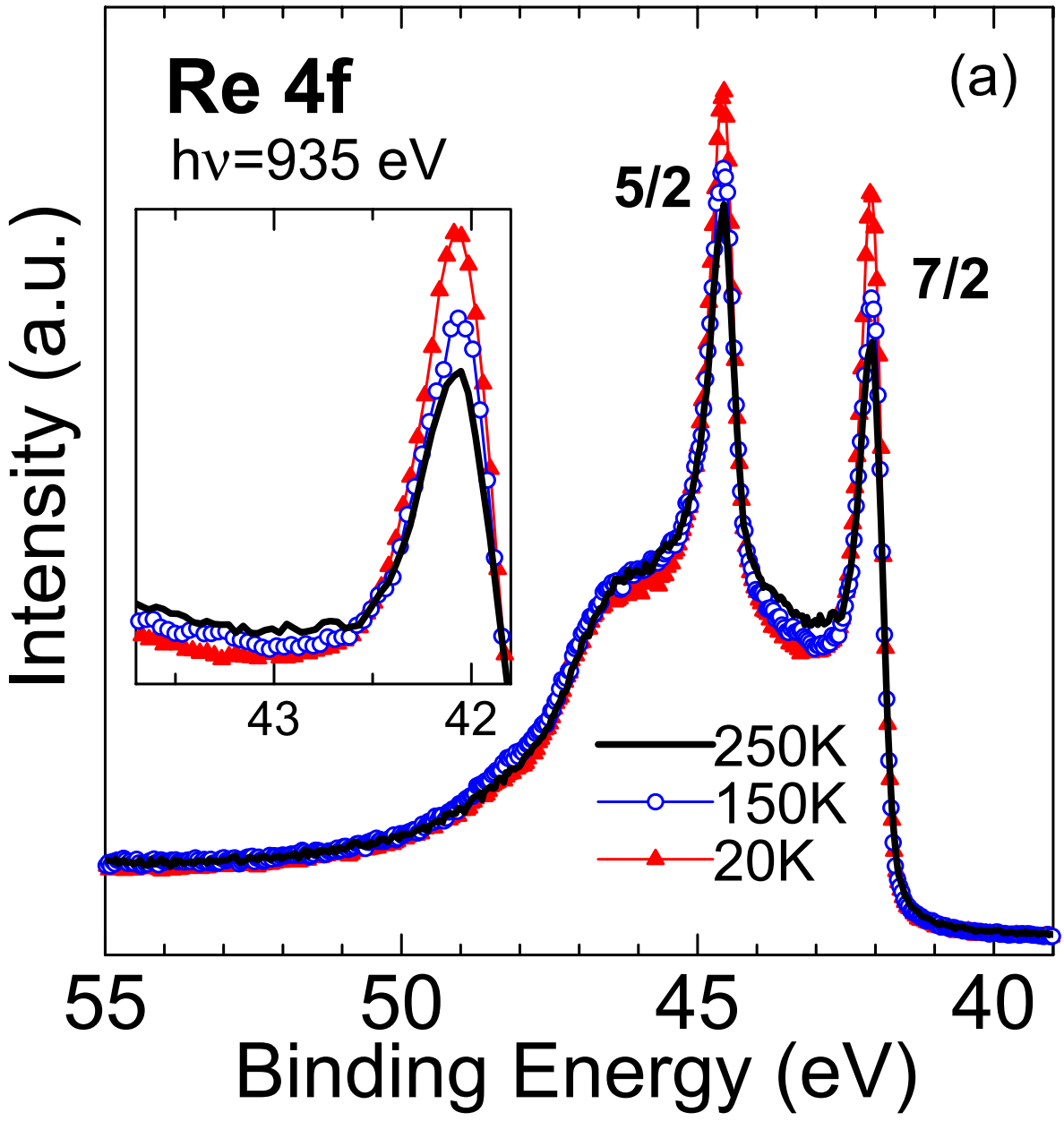
Re 4f
hν=935 eV
(a)
5/2
7/2
Intensity (a.u.)
43
42
250K
150K
20K
55
50
45
40
Binding Energy (eV)

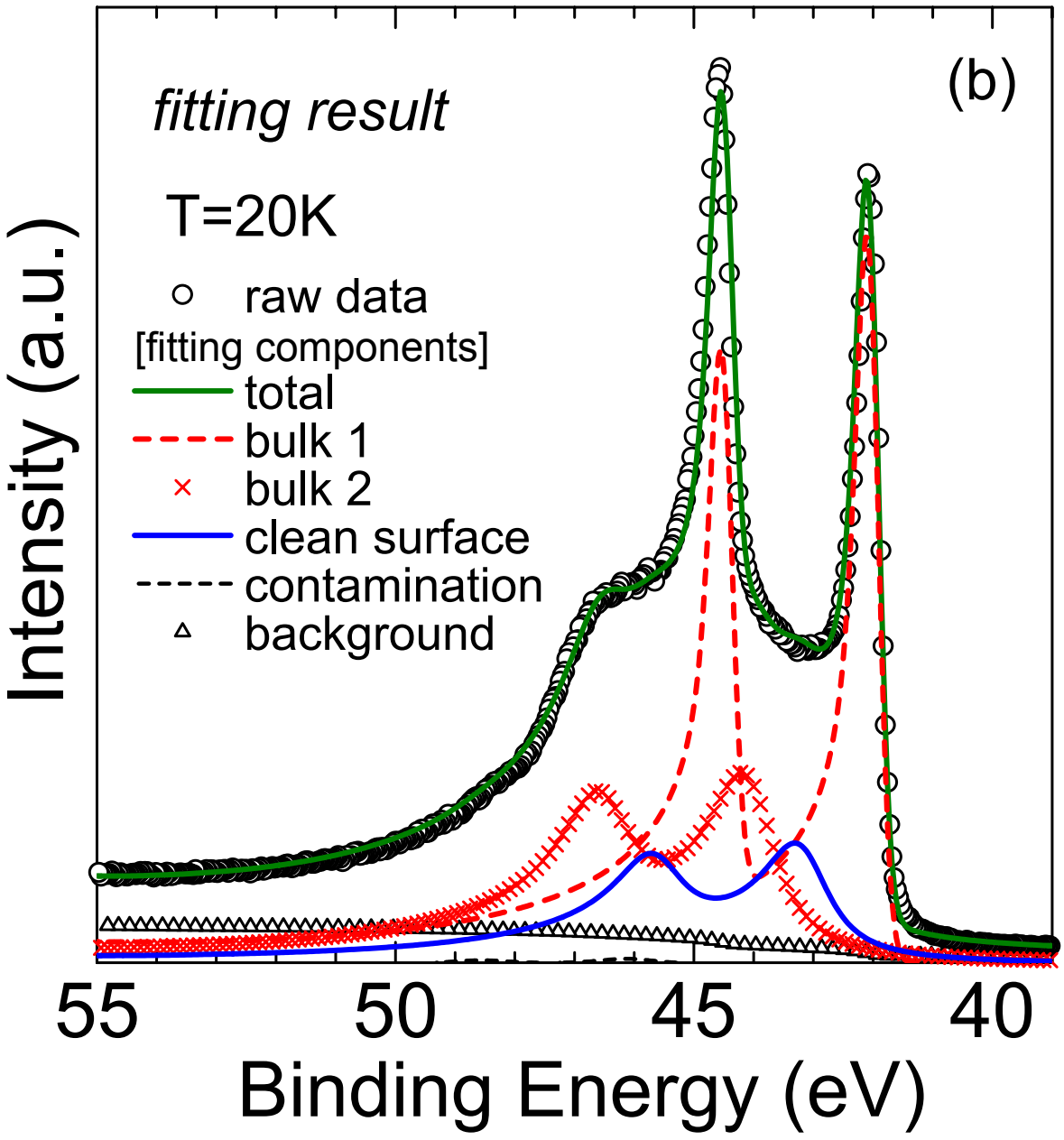
fitting result
T=20K
(b)
raw data
[fitting components]
total
bulk 1
bulk 2
clean surface
contamination
background
Intensity (a.u.)
55
50
45
40
Binding Energy (eV)

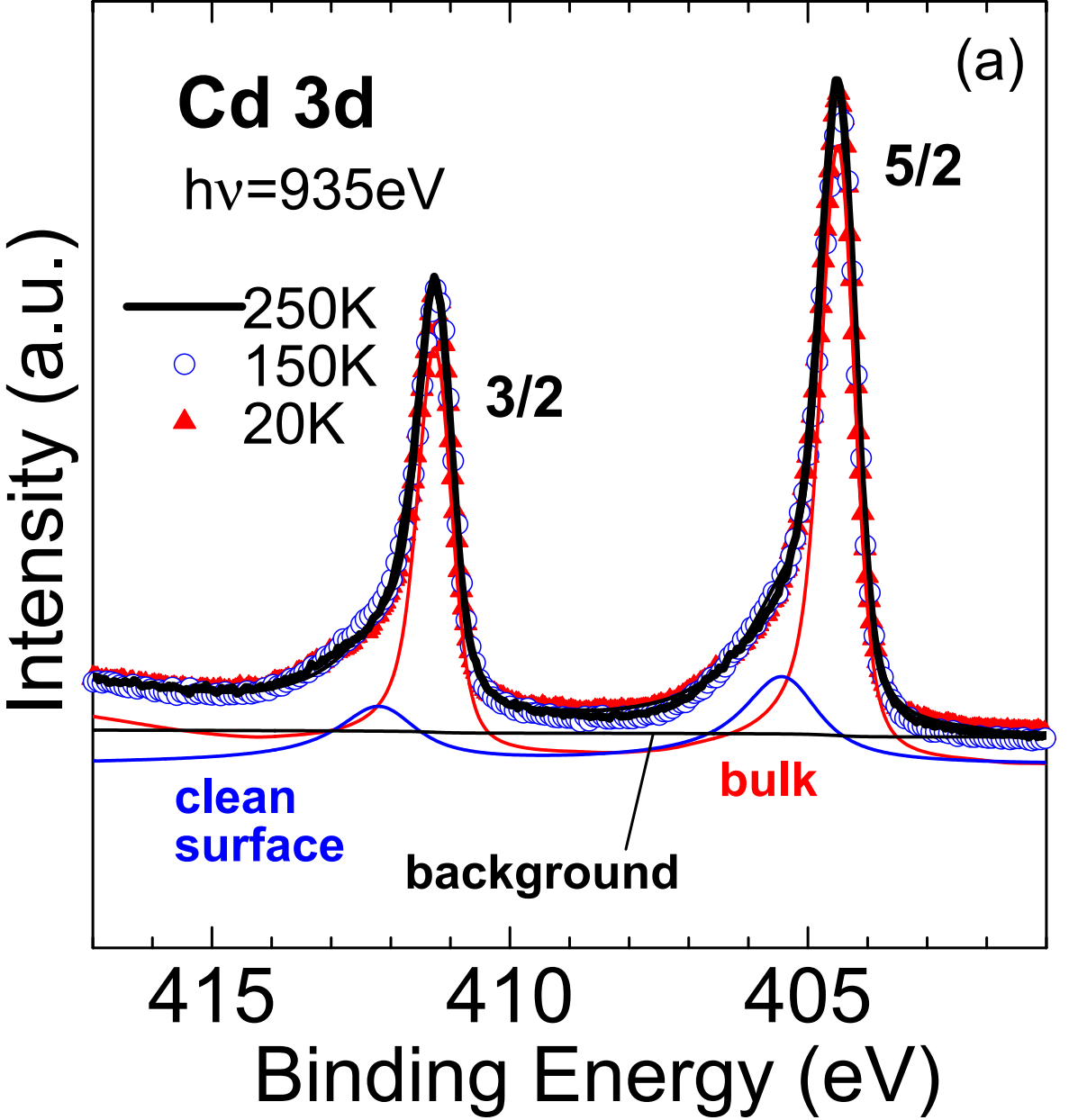
(a)
Cd 3d
hν=935eV
250K
150K
20K
3/2
5/2
clean
surface
bulk
background
Intensity (a.u.)
415
410
405
Binding Energy (eV)

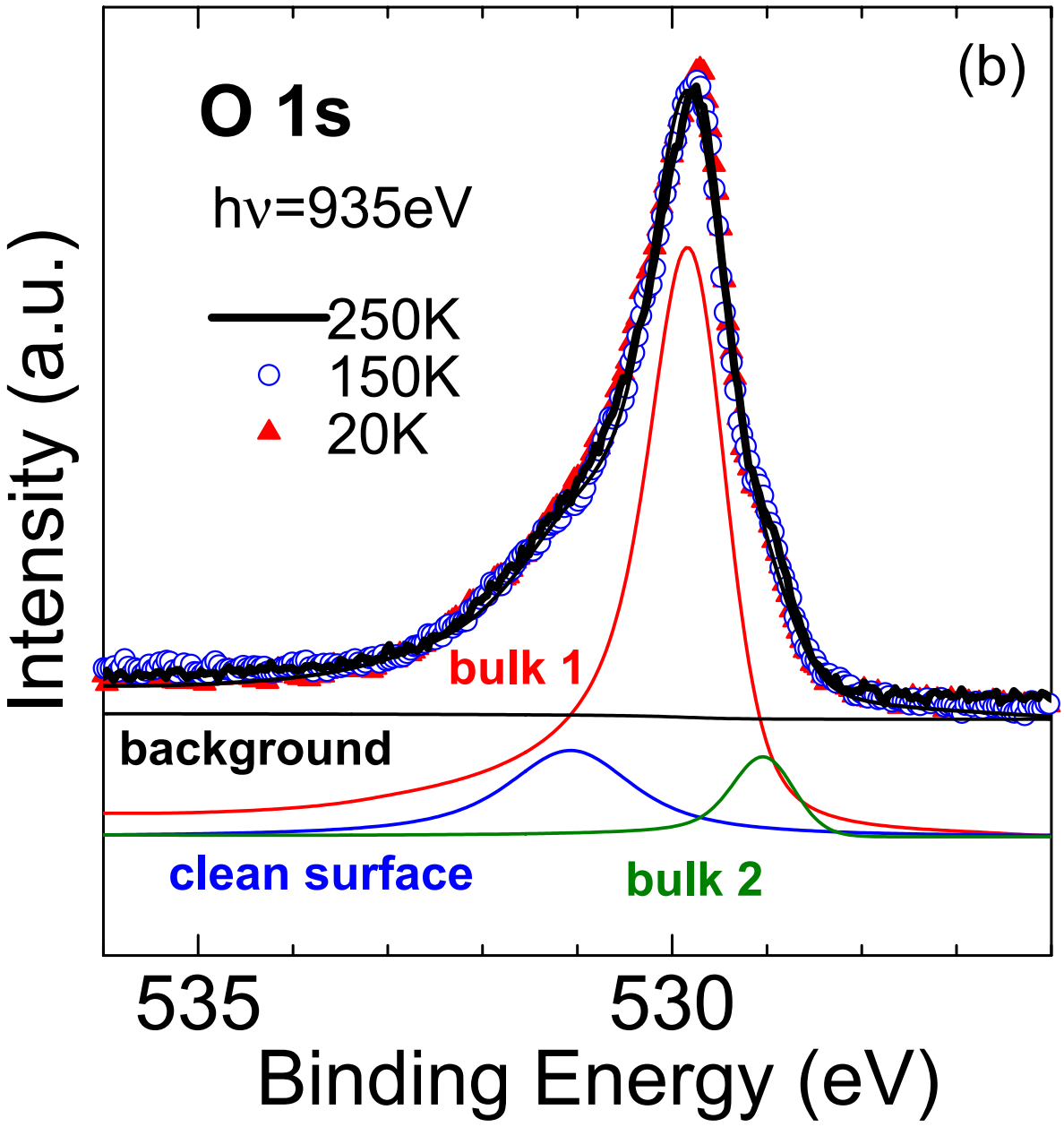
(b)
O 1s
hν=935eV
250K
150K
20K
bulk 1
background
clean surface
bulk 2
Intensity (a.u.)
535
530
Binding Energy (eV)

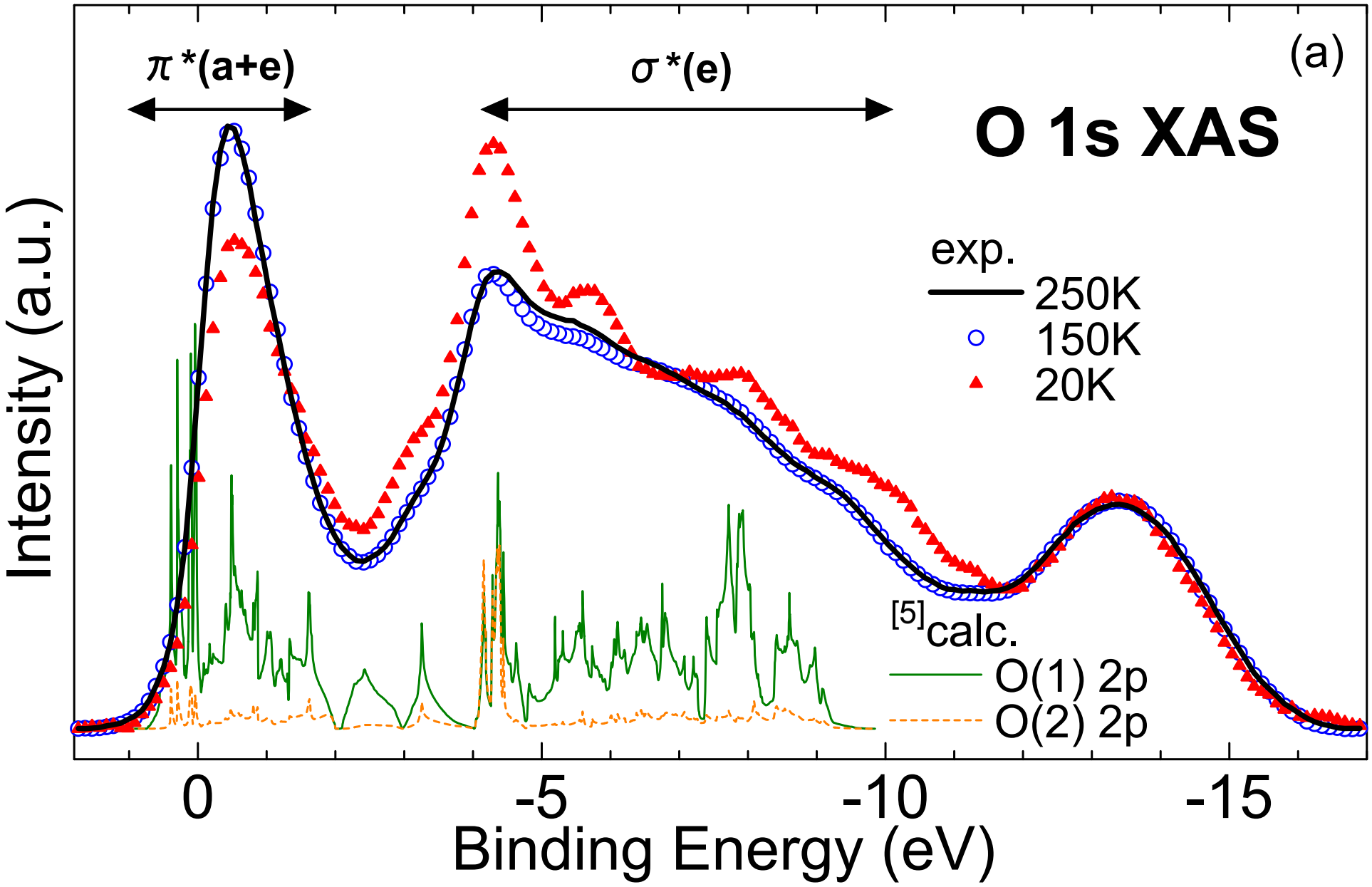
(a)
O 1s XAS
π*(a+e)
σ*(e)
Intensity (a.u.)
exp.
250K
150K
20K
[5]calc.
O(1) 2p
O(2) 2p
0
-5
-10
-15
Binding Energy (eV)

σ*(e)

π*(a+e)

Re 5d

E_F

π

σ

O 2p

(b)

250K

20K

O 1s XAS

PES

(Re 5d PDOS)